S100A8	S100 calcium binding protein A8
S100A9	S100 calcium binding protein A9
STZ	Streptozotocin
TLR	Toll-like receptor
TRIF	TIR-domain-containing adapter-inducing interferon-β
WT	Wild-type

Introduction

Diabetic nephropathy is one of the most prevalent causes of end-stage renal disease (ESRD) [1]. Despite progress in pharmacological strategies to control diabetes, hypertension and other metabolic abnormalities, the number of patients entering ESRD because of diabetic nephropathy remains extremely high, and the development of new classes of therapeutic reagents is eagerly anticipated [2]. During recent decades, the pathophysiology of diabetic nephropathy has become complex and serious because of coexisting lifestyle-related disorders, such as hyperlipidaemia, hypertension and obesity [3]. In fact, hyperlipidaemia is an independent risk factor for the progression of diabetic nephropathy in both type 1 and type 2 diabetes [4, 5], but the underlying molecular mechanism remains elusive [6].

Toll-like receptors (TLRs) are a family of receptors that play a critical role in the innate immune system by activating pro-inflammatory signalling pathways in response to molecular patterns synthesised by microorganisms [7]. TLR4, one of the best-characterised TLRs, binds with lipopolysaccharide from Gram-negative bacterial cell walls and with several endogenous ligands [7]. TLR4 also plays an important role in various kidney disorders, such as glomerulonephritis, renal ischaemia and diabetic tubular inflammation [8–13], but the role of TLR4 in diabetic glomerular injury and hyperlipidaemia-induced kidney damage remains largely unknown.

In the current study, TLR4 and its novel endogenous ligand S100 calcium binding protein A8 (S100A8) emerged as candidate molecules involved in the progression of diabetic nephropathy by our microarray analysis performed in two different types of diabetic mouse models. Furthermore, we examined the effects of high-fat diet (HFD) feeding on streptozotocin (STZ)-induced diabetes in *Tlr4* knockout (KO) and wild-type (WT) mice in order to elucidate the mechanism for the progression of diabetic nephropathy caused by hyperlipidaemia.

Methods

Experimental animals Male *Tlr4* KO [14] and WT mice with a C57BL/6 J genetic background were studied. To generate a mouse model of diabetes complicated by hyperlipidaemia, 8-week-old mice were intraperitoneally injected with STZ (100 mg/kg body weight in citrate buffer, pH 4.0; Sigma-Aldrich, St Louis, MO, USA) or vehicle for 3 consecutive days. After 2 weeks, normal diet (ND; NMF, 14.7 kJ/g [3.5 kcal/g], 13% of energy as fat; Oriental Yeast, Tokyo, Japan) was substituted with an HFD (D12451, 19.7 kJ/g [4.7 kcal/g], 45% of energy as fat; Research Diets, New Brunswick, NJ, USA) in subgroups of animals, and all were killed for analysis at 8 weeks after STZ treatment. In another set of experiments, 8-week-old male *db/db* mice (on a BKS genetic background; Japan Clea, Tokyo, Japan) were randomly assigned to ND or HFD (D12492, 21.8 kJ/g [5.2 kcal/g], 60% of energy as fat; Research Diets) groups and followed for 4 weeks. All animal experiments were conducted in accordance with the Guidelines for Animal Research Committee of Kyoto University Graduate School of Medicine.

Human biopsy samples Human kidney samples obtained at renal biopsy carried out in our department were used for immunohistochemistry. The human study protocol was approved by the Ethical Committee on Human Research of Kyoto University Graduate School of Medicine. All participants gave written informed consent.

Measurement of metabolic variables Metabolic variables were measured as described previously [15, 16]. Briefly, blood pressure was measured by indirect tail-cuff method (Muromachi Kikai, Tokyo, Japan). Urine samples were collected with metabolism cages, and urinary albumin was measured with competitive ELISA (Exocell, Philadelphia, PA, USA). Serum and urinary creatinine levels were assayed by enzymatic method (SRL, Tokyo, Japan) [17]. Plasma glucose, triacylglycerol and total cholesterol levels were measured, under conditions of ad libitum feeding, using an enzymatic method (Wako Pure Chemicals, Osaka, Japan). Plasma insulin levels were measured by enzyme immunoassay (Morinaga, Tokyo, Japan). For measurement of tissue triacylglycerol content, lipids were extracted with isopropyl alcohol/heptane (1:1 [vol./vol.]) from frozen kidney samples. After evaporating the solvent, lipids were resuspended in 99.5% ethanol and triacylglycerol contents were measured as described above.

Real-time quantitative RT-PCR Total RNA was extracted with TRIzol reagent (Invitrogen, Carlsbad, CA, USA) and cDNA in each sample was synthesised using the High Capacity cDNA Reverse Transcription Kit (Applied Biosystems, Foster City, CA, USA) from mouse kidneys and glomeruli isolated by graded sieving method [18, 19]. TaqMan real-time PCR was performed using Premix Ex Taq (Takara Bio, Otsu, Japan) and StepOnePlus Real Time PCR System (Applied Biosystems, Foster City, CA, USA). See Electronic supplementary material (ESM) Table 1 for primer

and probe sequences. Expression levels of all genes were normalised by *Gapdh* (internal control) levels. The mean expression level in whole kidney of WT non-treated control mice was arbitrarily defined as 1.0.

Histological analysis Periodic acid–Schiff (PAS) staining of the mesangial area and immunohistochemistry of S100A8 (requiring antigen retrieval by citrate buffer) and lectin, galactoside-binding, soluble, 3 (MAC-2 or LGALS3) [18] were carried out using kidney sections (thickness 4 μm) fixed with 4% buffered paraformaldehyde. Nuclei were counterstained with haematoxylin. All the primary antibodies used in this study are shown in ESM Table 2. For double staining, primary antibody for S100A8 was visualised with DyLight-conjugated secondary antibody (Takara Bio, Otsu, Japan). Immunofluorescence of podocin (or NPHS2) was performed with snap-frozen cryostat sections (4 μm), pretreated with cold acetone and 0.1% Triton-X100, and with primary and FITC-labelled secondary antibodies. Photographs were taken by a fluorescence microscope (IX81-PAFM; Olympus, Tokyo, Japan). Mesangial and podocin-positive areas of more than ten glomeruli from the outer cortex were measured quantitatively to obtain an average for each mouse using MetaMorph 7.5 software (Molecular Devices, Downingtown, PA, USA). Formalin-fixed, snap-frozen sections (10 μm) were stained with Oil Red O to evaluate lipid-droplet-positive areas.

Microarray analysis Two different types of diabetic mouse model were employed for microarray analysis. Male A-ZIP/F-1 heterozygous transgenic mice and control male FVB/N littermates were used at 10 months of age, when A-ZIP/F-1 mice exhibited diabetic nephropathy with massive proteinuria [20]. The other model was STZ-induced, insulin-dependent, diabetic C57BL/6 J male mice (Japan Clea) in which diabetes was induced at 9 weeks of age by single intraperitoneal injection of STZ (180 mg/kg); mice were analysed 8 weeks later. We essentially followed the procedures described in detail in the GeneChip Eukaryotic Target Preparation & Hybridization Manual (Affymetrix, Santa Clara, CA, USA). In brief, cDNA was synthesised and biotin-labelled cRNA was produced through in vitro transcription labelling Kit (Affymetrix). Fragmented cRNA was hybridised to GeneChip Mouse Genome 430 2.0 Array (Affymetrix) at 45°C for 16 h. The samples were washed and stained according to the manufacturer's protocol on GeneChip Fludisc Station 450 (Affymetrix) and scanned on GeneChip Scanner 3000 (Affymetrix).

PCR array analysis To eliminate contaminating genomic DNA, total RNA extracted from kidney samples was purified using RNeasy Mini Kit (QIAGEN Sciences, Maryland, MD, USA). First-strand cDNA was synthesised from total RNA using the RT2 first-strand kit (SABiosciences, Frederick, MD, USA). The mouse TLR-signalling pathway RT2 Profiler PCR plate (PAMM-018, SABiosciences) and StepOnePlus were used for amplification of cDNA. The analysis used 96 well plates containing gene-specific primer sets for 84 relevant TLR pathway genes, five housekeeping genes and two negative controls. The cycle threshold (C_t) was determined for each sample and normalised to the average C_t of the five housekeeping genes. The comparative ΔC_t method (SABiosciences) was used to calculate relative gene expression.

Western blot analysis Proteins extracted from kidney samples were separated by SDS-PAGE, transferred onto PVDF membranes, incubated with primary antibodies and detected with peroxidase-conjugated secondary antibodies and chemiluminescence [19]. Glyceraldehyde-3-phosphate dehydrogenase (GAPDH) was used as an internal control.

Cultured macrophages Palmitate (Sigma-Aldrich) was solubilised in ethanol, and combined with fatty-acid-free, low endotoxin, bovine serum albumin (Sigma-Aldrich) at a molar ratio of 10:1 in serum-free medium. Polymyxin B (10 μg/ml, Nacalai Tesque, Kyoto, Japan) was added to each well to minimise contamination of endotoxin. Bone marrow-derived macrophages (BMDMs) were generated from mice as described previously [21]. Briefly, following lysis of erythrocytes, bone marrow cells were resuspended in medium containing 20% fetal calf serum and 50 ng/ml recombinant human macrophage colony-stimulating factor, and cultured at 37°C in 5% CO_2 atmosphere. On day 6, the medium was replaced with fresh medium containing 5.6 mmol/l or 25 mmol/l glucose. On day 7, macrophages were incubated with palmitate or vehicle for 24 h. Total RNA from cells was extracted with RNeasy Mini Kit, and mRNA expression levels of *S100a8* and *Tlr4* were determined by TaqMan real-time RT-PCR.

Statistical analysis Data are expressed as means±SEM. Differences between multiple groups were assessed by two-way factorial ANOVA with Bonferroni's post test. Comparisons between two groups were carried out by unpaired Student's *t* test. Statistical significance was defined as $p<0.05$.

Results

Changes of metabolic variables and albuminuria in WT diabetic mice given a fat-rich diet Metabolic variables of non-STZ (nSTZ)-HFD, STZ-ND, STZ-HFD and control nSTZ-ND groups of WT mice are shown in Table 1. HFD treatment (compared with ND) in nSTZ mice caused significant elevation of body weight, plasma glucose, insulin,

Table 1 Metabolic data of WT and *Tlr4* KO mice at 8 weeks after STZ injection

Variable	WT				KO			
	nSTZ-ND	nSTZ-HFD	STZ-ND	STZ-HFD	nSTZ-ND	nSTZ-HFD	STZ-ND	STZ-HFD
Number of animals	6	4	8	11	4	4	5	8
Body weight (g)	27.7±1.0	33.7±0.5**	20.0±0.9**	22.1±0.5**,§§§	34.9±2.4†	39.6±1.4†	22.0±1.3**	23.3±0.6***,§§§
Blood pressure (mmHg)								
Systolic	101±2	104±2	98±1	100±1	103±2	103±2	96±1*	101±2
Diastolic	56±2	57±3	52±2	56±2	55±1	57±2	50±1*	53±1
Kidney weight (% body weight)	0.5±0.0	1.0±0.0**	1.7±0.1**	1.8±0.1**,§§§	1.0±0.1†††	2.2±0.2***,††	1.9±0.2***	1.9±0.1***
Plasma glucose (mmol/l)	9.5±1.6	14.0±0.4*	40.0±3.9**	32.9±1.8**,§	10.4±1.1	12.7±2.3	36.0±7.7*	31.8±2.3***,§§
HbA_{1c} (%)	3.4±0.1	5.3±0.1**	9.6±0.6**	9.9±0.5**,§	3.0±0.3	4.9±0.2**	9.4±1.1**	10.3±0.3***,§§§
HbA_{1c} (mmol/mol)	13.3±1.4	34.1±0.7**	81.8±6.5**	84.6±5.1**,§	9.0±2.8	29.5±2.5**	78.9±12.5**	89.4±3.2***,§§§
Plasma insulin (pmol/l)	133±16	256±21**	10±2**	12±2**,§§§	238±43	336±33	12±5**	12±5**,§§§
Plasma triacylglycerol (mmol/l)	0.99±0.02	1.20±0.03**	2.36±1.01*	5.48±1.56*,§	1.74±0.32	1.42±0.11	3.12±1.56	7.64±1.58**,§§
Plasma total cholesterol (mmol/l)	1.5±0.4	3.4±0.3*	5.1±0.8*	5.2±0.5**	1.9±0.4	3.4±0.2*	3.8±0.6*	5.9±0.4**,§§,‡
Serum creatinine (μmol/l)	8.0±1.8	8.8±0.1	10.6±0.9	15.9±5.3	8.8±0.1	8.0±0.1††	10.6±1.8	8.0±0.1

Data are means±SEM

Blood was collected with mice fed ad libitum

*$p<0.05$, **$p<0.01$, ***$p<0.001$ vs nSTZ-ND; †$p<0.05$, ††$p<0.01$, †††$p<0.001$ vs similarly treated group of WT; ‡$p<0.05$ vs STZ-ND; §$p<0.05$, §§$p<0.01$, §§§$p<0.001$ vs nSTZ-HFD

triacylglycerol and total cholesterol levels. STZ treatment (compared with nSTZ) in ND mice caused significant body weight loss and significant elevation of plasma glucose, triacylglycerol and total cholesterol levels. Treatment of STZ mice with HFD resulted in large exacerbation of hypertriacylglycerolaemia (by 2.3-fold) without significant changes in other above-mentioned variables (Table 1). Consistently, renal lipid deposition in STZ-HFD mice was markedly increased compared with STZ-ND mice (Fig. 1a, b). Blood pressures were not significantly different among the four treatment groups (Table 1).

Concerning albuminuria, one of the representative abnormalities that characterise diabetic nephropathy [2], albumin excretion in STZ-ND was elevated by 2.3-fold at 8 weeks compared with nSTZ-ND mice (Fig. 1c). The addition of HFD to STZ mice further enhanced albuminuria approximately twofold. To investigate podocyte injury, we investigated whether podocin protein production is decreased in the glomeruli of STZ-HFD mice [19]. Glomerular podocin level was significantly reduced in STZ-ND compared with nSTZ-ND and was lowest in STZ-HFD (Fig. 1e, f). Also, in obese, type 2 diabetic *db/db* mice, albuminuria was exaggerated by HFD (ESM Fig. 1). To summarise, treatment of WT mice with a combination of HFD and STZ resulted in marked enhancement of hypertriglycerolaemia, renal lipid deposition, podocyte damage and albumin excretion.

Gene expression analysis of pro-inflammatory and extracellular-matrix-associated genes in whole kidney and glomeruli and histological examination We measured mRNA levels of pro-inflammatory and extracellular matrix (ECM)-associated genes both in whole kidney and isolated glomeruli (Fig. 2, ESM Table 3). The former set of genes included *Mcp1* (also known as *Ccl2*, encoding monocyte chemoattractant protein-1 [MCP1]), *F4/80* (also known as *Emr1*), *Cd68*, *Tnfa* (also known as *Tnf* [encoding TNF]), *Pai1* (also known as *Serpine1* [encoding plasminogen activator inhibitor-1]) and *Il1b* (encoding IL1β). The latter set comprised *Tgfb1* (encoding TGFβ1), *Fn* (also known as *Fn1* [encoding fibronectin]), *Col4a3* (encoding type IV collagen alpha 3 chain), *Ctgf* (encoding connective tissue growth factor [CTGF]) and *Mmp2* (encoding matrix metalloproteinase 2). We found that expression levels of these genes in glomeruli and whole kidney were mildly elevated in WT STZ-ND compared with WT nSTZ-ND mice, in general (Fig. 2, ESM Table 3). Gene expression levels were further upregulated in WT STZ-HFD animals. Of note, differences between nSTZ-HFD and nSTZ-ND groups were

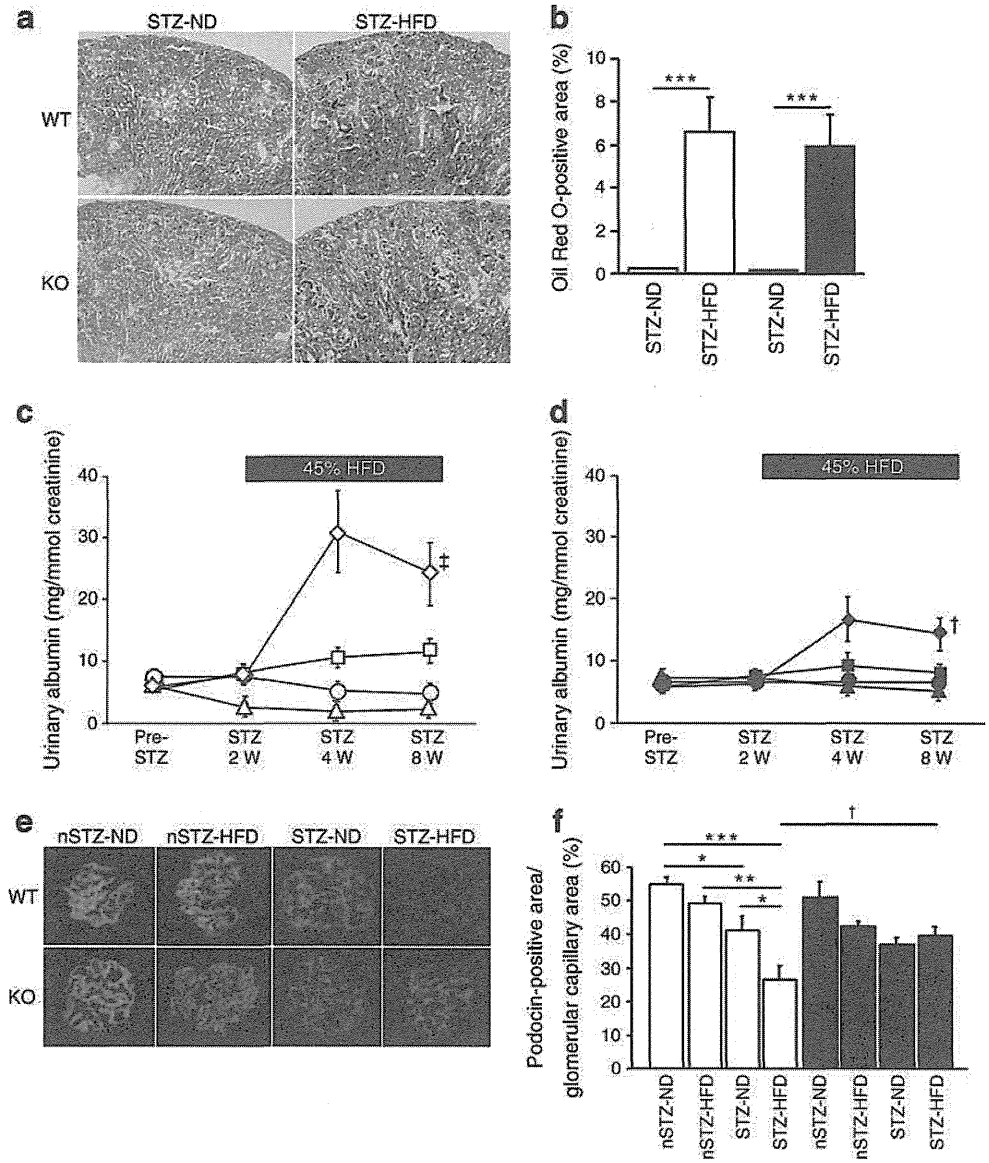

Fig. 1 Treatment of STZ diabetic mice with an HFD worsens renal injury in WT but not in *Tlr4* KO mice. (**a**, **b**) Addition of HFD to STZ mice causes similar degrees of deposition of lipid droplets staining positive with Oil Red O in WT (white bars) and KO mice (black bars) at 16 weeks of age. Magnification×4. Data are means±SEM. $n=5$. ***$p<0.001$. Time course of urinary albumin levels normalised with urinary creatinine levels in WT (**c**) and *Tlr4* KO mice (**d**). Circles, nSTZ-ND; triangles, nSTZ-HFD; squares, STZ-ND; diamonds, STZ-HFD. W, weeks after STZ injection. $n=6$–10. $^{‡}p<0.05$ vs WT STZ-ND, $^{†}p<0.05$ vs WT STZ-HFD calculated by area under the curve. (**e**, **f**) Immunofluorescence analysis of glomerular podocin level. White bars, WT; black bars, KO; $n=4$–6. *$p<0.05$, **$p<0.01$, ***$p<0.001$. $^{†}p<0.05$ for similarly treated KO vs WT

negligible (Fig. 2). Histological analysis also showed that MAC-2-positive-macrophage infiltration into glomeruli (Fig. 3a) and renal interstitium (ESM Fig. 2) and glomerular mesangial expansion (Fig. 3b) in STZ-HFD mice were markedly more pronounced than in STZ-ND mice.

Screening of candidate genes involved in the pathogenesis of diabetic nephropathy To identify candidate molecules potentially involved in the pathophysiology of diabetic nephropathy, we analysed gene expression profiles of diabetic mouse glomeruli by microarray (ESM Table 4). We compared two types of diabetic nephropathy from STZ-induced and A-ZIP/F-1 lipoatrophic diabetes mice. We selected commonly regulated genes to minimise interference from the renal toxicity of STZ, genetic background [22] and direct insulin or leptin target molecules [23]. The list of genes commonly upregulated in these two models included pro-inflammatory and ECM-associated genes and also ones encoding TLRs (ESM Table 4). As pairs of cell surface receptors and their ligands provide attractive seeds for future therapeutic targets, we focused on TLR4, for which glomerular levels were elevated by 1.7-fold by STZ and 5.8-fold in A-ZIP/F-1 compared with each control by microarray. We further examined the expression of genes encoding molecules reported to be endogenous ligands for TLR4 [7], and identified *S100a8* (also known as *Mrp8*) and *S100a9* (also known as *Mrp14*]) [24], for which glomerular gene expression was commonly upregulated in two models of diabetic nephropathy by microarray (ESM Table 4). Upregulation of *Tlr4* and *S100a8* gene expression in glomeruli of STZ and A-ZIP/F-1 mice was confirmed by quantitative RT-PCR (ESM Fig. 3a, b). Moreover, in STZ-HFD mice, expression of these genes was further potentiated compared with other groups such as STZ-ND and nSTZ-HFD, especially in

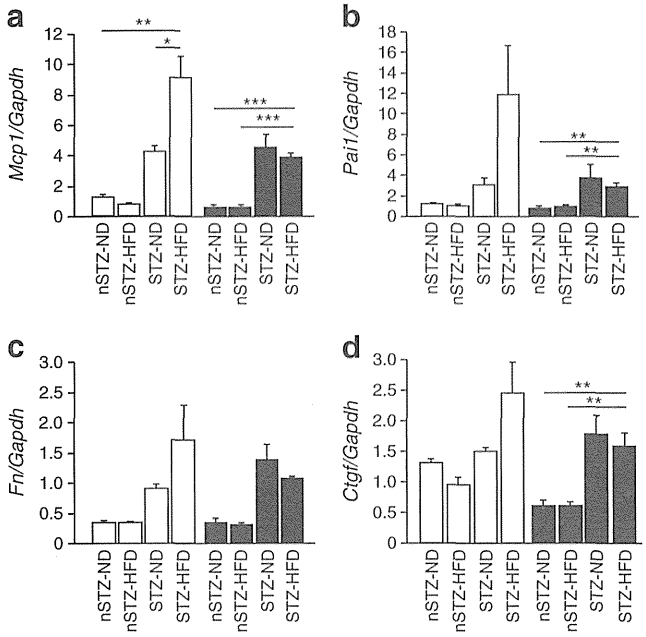

Fig. 2 Treatment with STZ and HFD synergistically upregulates inflammatory and ECM-associated gene expression in glomeruli of WT mice by real-time RT-PCR, but the effects of HFD are largely blunted in *Tlr4* KO mice: (**a**) *Mcp1*; (**b**) *Pai1*; (**c**) *Fn*; and (**d**) *Ctgf*. White bars, WT; black bars, KO. Data are means±SEM. n=4–11. *p<0.05, **p<0.01, ***p<0.001

glomeruli (Fig. 4a), but not in whole kidney (ESM Fig. 4). However, there was no significant increase in the expression of genes encoding other endogenous ligands for TLR4, such as *Hmgb1*, at the same time in both STZ and A-ZIP/F-1 mice compared with their respective controls, as assessed by microarray (ESM Table 4) or by quantitative RT-PCR (ESM Fig. 3c, d).

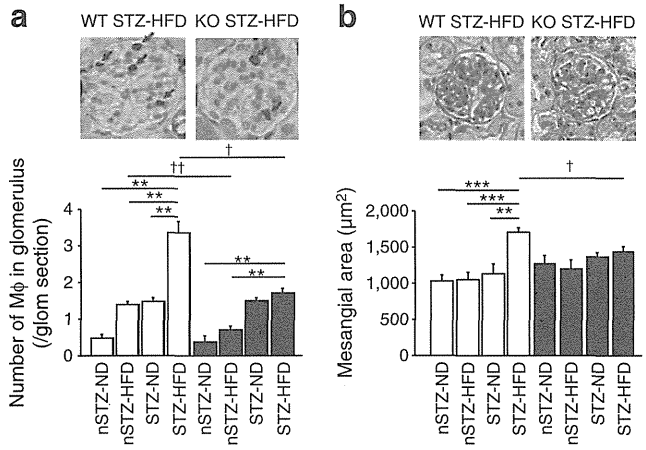

Fig. 3 Glomerular macrophage infiltration and mesangial matrix accumulation are markedly enhanced in WT mice co-treated with STZ and HFD, but not in *Tlr4* KO mice. **a** Macrophage (Mϕ) number per glomerular (glom) section determined by MAC-2 immunostaining (arrows). Magnification ×40. Data are means±SEM. n=4–5. **b** Glomerular mesangial area determined by PAS staining (purple). Magnification ×20. n=4–6. White bars, WT; black bars, KO. **p<0.01, ***p<0.001. $^{\dagger}p$<0.05, $^{\dagger\dagger}p$<0.01 for similarly treated KO vs WT

Production of S100A8 protein in diabetic kidney We performed immunohistochemical analyses of S100A8 protein in the kidneys both in STZ-HFD mice and human biopsy samples. In mice, abundance of S100A8 protein, in a punctate pattern, was observed predominantly in glomeruli of WT STZ-HFD mice, while S100A8 abundance was much lower in glomeruli of nSTZ-ND, nSTZ-HFD and STZ-ND groups (Fig. 4b, ESM Fig. 5). S100A8 protein was also detected in the interstitium of STZ-HFD mice but less abundantly than in the glomeruli. Double immunostaining revealed that 86% of S100A8 signals co-localised with macrophage marker MAC-2 in the glomeruli of STZ-HFD mice (Fig. 4c). In humans, S100A8 was abundantly detected in the glomeruli of patients with diabetic nephropathy, but not obviously in glomeruli of minor glomerular abnormality or minimal change nephrotic syndrome cases (Fig. 5).

Effects of Tlr4 defect on STZ-HFD mice and on BMDMs To elucidate a functional role played by TLR4 in the progression of diabetic nephropathy accelerated by diet-induced hyperlipidaemia, we investigated the effects of STZ and HFD in *Tlr4* KO mice. In baseline nSTZ-ND conditions, KO mice showed significantly heavier body weights compared with WT mice, paralleled by mildly elevated plasma levels of glucose, insulin, triacylglycerol and total cholesterol in KO mice (Table 1). Plasma glucose levels in KO nSTZ-HFD mice were slightly lower compared with their WT counterparts. These findings are consistent with previous observations indicating that, compared with WT mice, *Tlr4* KO mice are prone to accumulation of fat but resistant to development of insulin resistance when challenged with an HFD [25, 26]. When STZ-HFD conditions were compared between KO and WT mice, the levels of plasma glucose and total cholesterol and renal lipid deposition were similar among the genotypes, and plasma triacylglycerol levels tended to be higher in KO than WT mice (Table 1, Fig. 1b). On the other hand, exacerbation of albuminuria and suppression of glomerular podocin protein production resulting from HFD treatment in WT STZ mice were all largely blunted in KO STZ animals (Fig. 1c–f). Additionally, infiltrated macrophage counts in glomeruli and renal interstitium and mesangial expansion were remarkably smaller in KO STZ-HFD mice than in WT STZ-HFD mice (Fig. 3, ESM Fig. 2). Furthermore, upregulation of pro-inflammatory (*Mcp1* and *Pai1*), pro-fibrotic (*Fn* and *Ctgf*), *S100a8* and *S100a9* gene expression and S100A8-positive cell counts caused by HFD treatment in glomeruli of WT STZ mice were almost completely abolished in KO STZ mice (Figs 2 and 4a, b, ESM Fig. 5). These findings indicate that, despite similar degrees of metabolic abnormalities caused

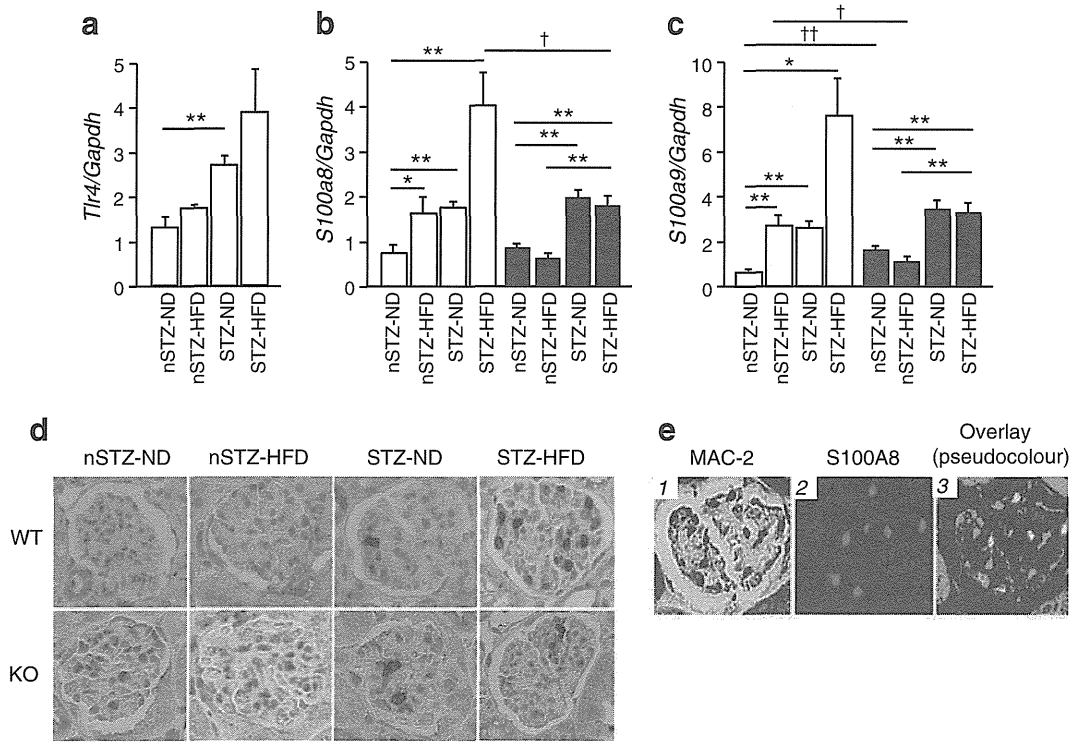

Fig. 4 Glomerular expression of *Tlr4*, *S100a8* and *S100a9* mRNA and S100A8 protein is markedly upregulated in WT STZ-HFD but not in *Tlr4* KO STZ-HFD mice, and S100A8 is predominantly produced by glomerular macrophages in WT STZ-HFD mice. **a–c** Gene expression of *Tlr4* (**a**), *S100a8* (**b**) and *S100a9* (**c**) in glomeruli, determined by real-time RT-PCR. White bars, WT; black bars, KO. Data are means± SEM. n=4–11. *p<0.05, **p<0.01. $^{\dagger}p$<0.05, $^{\dagger\dagger}p$<0.01 for similarly treated KO vs WT. **d** Glomerular S100A8 protein (brown) examined by immunohistochemistry. Magnification×40. **e** Localisation of MAC-2 (brown in panel 1, pseudocoloured with green in panel 3, by immunohistochemistry), S100A8 (red in panels 2 and 3, by immunofluorescence) and their overlaps (yellow in panel 3) in glomeruli of WT STZ-HFD mice

by diabetes and hyperlipidaemia, *Tlr4* KO mice developed much less severe renal lesions compared with WT mice.

With regard to comparison between WT and *Tlr4* KO mice treated with STZ alone (STZ-ND mice), urinary albumin excretion (Fig. 1c, d), glomerular podocin production (Fig. 1e, f), glomerular gene expression of *Mcp1*, *Pai1*, *Fn*, *Ctgf*, *S100a8*, and *S100a9* (Figs 2 and 4a), and glomerular macrophage infiltration (Fig. 3a) were all similar among two genotypes, suggesting that *Tlr4* does not strongly participate in early and mild changes of diabetic nephropathy. Concerning HFD treatment alone (nSTZ-HFD mice), there were no significant differences in urinary albumin excretion and glomerular podocin production between WT and KO mice (Fig. 1c–f), while glomerular *S100a9* gene expression (Fig. 4a) and glomerular macrophage infiltration (Fig. 3a) were significantly attenuated in KO compared with WT mice, suggesting that treatment solely with HFD significantly activated circulating macrophages in WT mice but the TLR4-mediated signal in nSTZ-HFD mice was not sufficient to cause functional changes in the glomeruli.

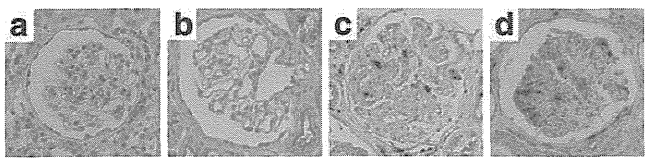

Fig. 5 S100A8 (brown) is observed in glomeruli of patients with diabetic nephropathy by immunohistochemistry: (**a**) minor glomerular abnormality; (**b**) minimal change nephrotic syndrome; and (**c**) mild and (**d**) severe cases of diabetic nephropathy

To gain insights into how the combination of diabetes and hyperlipidaemia resulted in markedly enhanced migration of macrophages into glomeruli, we examined BMDMs. We focused attention on expression of a potent TLR4 ligand, S100A8 [24]. Treatment of WT macrophages with a fatty acid, palmitate, induced *S100a8* mRNA upregulation when the cells were cultured in high-glucose conditions, but upregulation was not observed under low-glucose conditions (Fig. 6a). Furthermore, induction of *S100a8* expression by palmitate in high-glucose-treated macrophages did not occur in cells from *Tlr4* KO animals (Fig. 6b). High-glucose treatment slightly increased *Tlr4* expression in WT macrophages (Fig. 6c).

TLR4 signalling in the kidney of STZ-HFD model To examine the TLR4-downstream signalling cascade, we performed

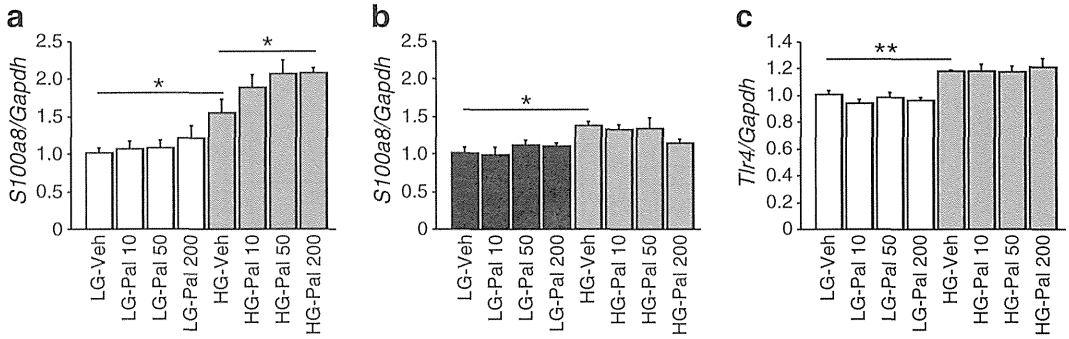

Fig. 6 *S100a8* expression in BMDMs is synergistically induced by high glucose and palmitate in a *Tlr4*-dependent manner. **a** *S100a8* mRNA expression by real-time RT-PCR in BMDMs from WT mice cultured under low-glucose (5.6 mmol/l, white bars) or high-glucose (25 mmol/l, grey bars) conditions and effects of palmitate (10–200 μmol/l). Data are means±SEM. $n=6$. **b** *S100a8* mRNA expression in BMDMs from *Tlr4* KO mice cultured under low-glucose (black bars) or high-glucose (grey bars) conditions and the effects of palmitate. $n=6$. **c** *Tlr4* mRNA expression in WT BMDMs. $n=6$. $^*p<0.05$, $^{**}p<0.01$. LG, low glucose; HG, high glucose; pal, palmitate; Veh, vehicle

western blot analyses of key adaptor proteins and transcription factors which have been reportedly classified into myeloid differentiation primary response gene (88) (MYD88)-dependent, TIR-domain-containing adapter-inducing interferon-β (TRIF)-dependent or common pathways (Fig. 7a) [7], using whole kidney lysate. Treatment of WT STZ mice with HFD was associated with increased phosphorylation of inhibitor of κB (IKB) and c-Jun N-terminal kinase (JNK) in a common pathway, and with increased phosphorylation of interferon regulatory factor 3 (IRF3) in a TRIF-dependent pathway, but not with increased protein production of TNF receptor-associated factor 6 (TRAF6) nor increased phosphorylation of interleukin-1-receptor-associated kinase (IRAK) in the MYD88-dependent pathway (Fig. 7b–e). PCR array analysis, which allows simultaneous evaluation of relevant genes involved in the signalling cascades of TLR1–TLR9, confirmed that in WT STZ-HFD kidneys, TRIF-dependent pathway-inducible genes (*Cxcl10*, *Ifnb1* [encoding interferon β1] and *Cd80*) and common pathway-inducible genes (*Mcp1*) were highly upregulated, but genes involved in the MYD88-dependent pathway (*Cd14*, *Ly96* [encoding myeloid differentiation protein-2 {MD-2}], and *Traf6*) were not changed compared with WT STZ-ND kidneys (ESM Table 5). Furthermore, disruption of the *Tlr4* gene markedly blocked the activation of the putative TLR4 downstream signalling cascade in STZ-HFD mice (Fig. 7b–e, ESM Table 5).

Discussion

In the present study, we have revealed that treatment of WT mice with STZ combined with HFD synergistically aggravated renal lesions, indicated by enhancement of albuminuria, macrophage infiltration, mesangial expansion and pro-inflammatory/ECM-associated gene induction in glomeruli. These changes were accompanied with upregulation of a TLR4 ligand, S100A8, and activation of putative TRIF-dependent pathway downstream of TLR4. In *Tlr4* KO mice, the addition of HFD to STZ had almost no effect on kidney damage, suggesting that TLR4 plays an important role in the exacerbation of diabetic nephropathy by hyperlipidaemia.

Of note, treatment with STZ alone caused similar and mild renal changes in WT and KO mice, suggesting that the TLR4 signal may not significantly participate in the onset of diabetic nephropathy at 8 weeks after STZ injection [13]. However, WT mice fed with HFD (nSTZ-HFD) exhibited significantly higher levels of *S100a9* gene expression and more macrophage infiltration in glomeruli compared with KO mice, but these effects were not reflected in differences in other renal lesion variables, suggesting that macrophage activation in nSTZ-HFD mice may require longer observation periods than were used in this study in order to be functionally relevant.

Here, to study the effects of an HFD on diabetes, we used a lean model of type 1 diabetes to avoid introducing complexity through alterations in insulin resistance and fat accumulation with the HFD or by *Tlr4* gene disruption in the type 2 diabetes model [19, 20]. The HFD-induced and hypertriacylglycerolaemia-associated renal injury observed in this study may have been caused through activation of TLR4 by NEFA [25, 26], oxidised LDL [27], or triacylglycerol-rich lipoproteins [6]. Previous studies have proposed that, by direct lipotoxicity on tubular epithelial cells, diet-induced obesity alone is sufficient to cause inflammatory and fibrotic changes in the whole kidney preparations through gene expression of *Cd36* or *sterol regulatory element-binding protein-1c* (*Srebp1c*) [28–30]. In the present study, however, treatment of WT mice solely with HFD resulted in very mild renal lesions, probably because we used a diet with a lower fat content and studied the mice for a shorter period of time compared with earlier reports [28–30]. Furthermore, HFD increased glomerular *Cd36* mRNA expression but STZ-induced

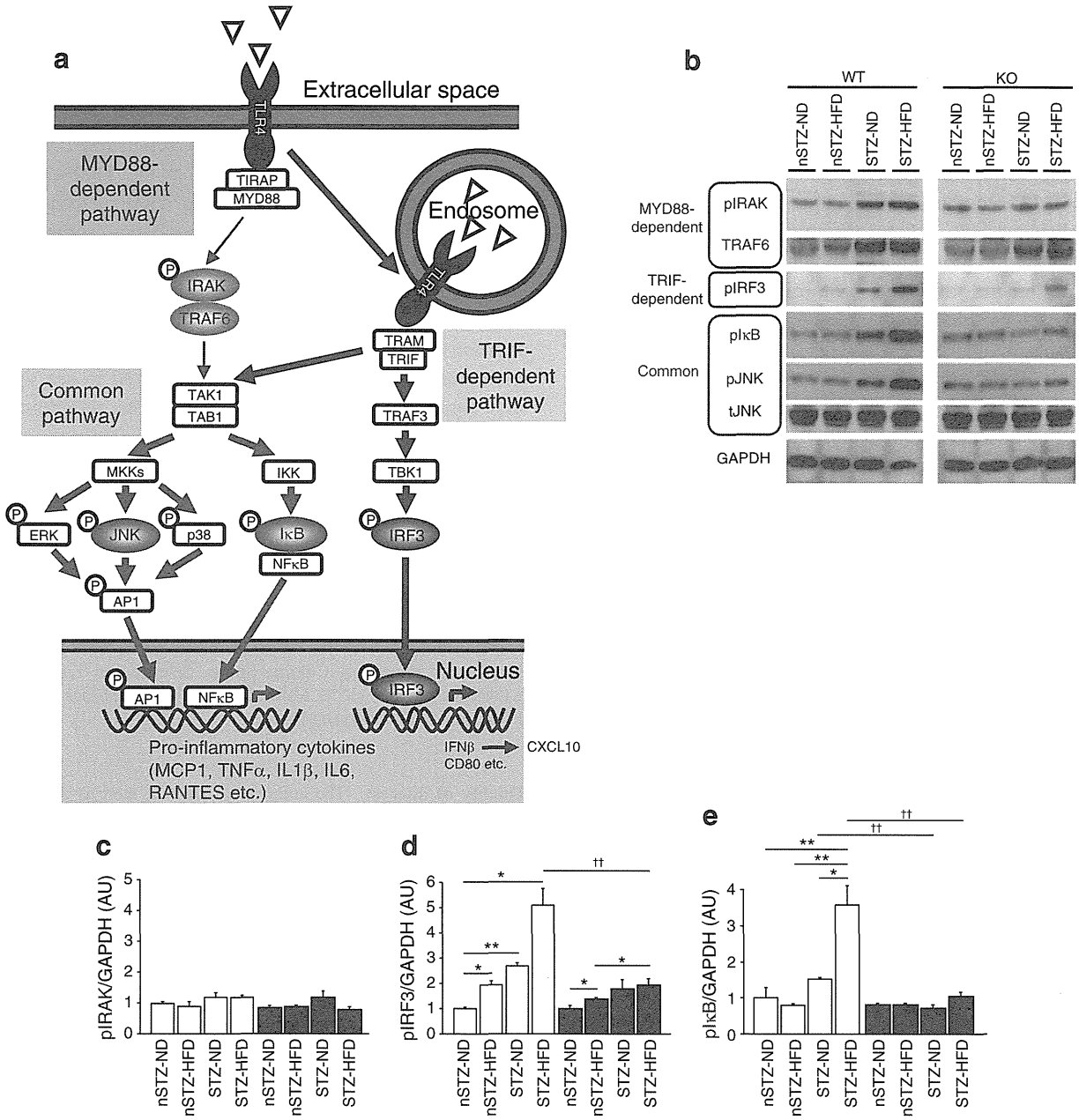

Fig. 7 Exacerbation of STZ-induced diabetic nephropathy by HFD is associated with increased phosphorylation of proteins involved in TRIF-dependent and common pathways of the TLR4 signalling cascade in WT kidney but not in *Tlr4* KO kidney. **a** Schema describing the known TLR4 signalling cascade. The common pathway can be activated both through MYD88-dependent and TRIF-dependent pathways. Key molecules analysed in (b) are highlighted as elliptical objects. **b-e** Western blot analyses of TLR4 signalling and quantitative evaluation. White bars, WT; black bars, KO. Data are means±SEM. n=4. *p<0.05, **p<0.01. $^{\dagger\dagger}p$<0.01 for similarly treated KO vs WT. AP1, jun proto-oncogene; AU, arbitrary units; CXCL10, chemokine (C-X-C motif) ligand 10; ERK, mitogen-activated protein kinase 1; (p)IKB, (phosphorylated) inhibitor of κB ; IKK, inhibitor of kappa light polypeptide gene enhancer in B cells, kinase; (p)IRAK, (phosphorylated) interleukin-1 receptor-associated kinase 1; pIRF3, phosphorylated IRF3; (p)/(t)JNK, (phosphorylated)/(total) JNK; MKKs, mitogen-activated protein kinase kinases; p38, mitogen-activated protein kinase 14; RANTES, chemokine (C-C motif) ligand 5; TAB1, TGFβ-activated kinase 1/MAP3K7 binding protein 1; TAK1, nuclear receptor subfamily 2, group C, member 2; TBK1, TANK-binding kinase 1; TIRAP, Toll-interleukin 1 receptor domain containing adaptor protein; TRAF3, TNF receptor-associated factor 3; TRAM, translocation associated membrane protein 1

diabetes reduced it, and glomerular *Srebp1c* expression was decreased both by HFD and STZ (ESM Fig. 6), indicating that HFD-induced exacerbation of diabetic nephropathy cannot be explained by upregulation of CD36 or SREBP1C.

S100A8 forms a heterodimer with S100A9, and the complex is one of the most powerful endogenous ligands for TLR4, which is essential for full activation of macrophages and other leucocytes, by a positive feedback loop, during

endotoxin-induced shock and vascular and autoimmune disorders [24, 31, 32]. TLR4 signalling also plays an important role in the development of various kidney diseases, yet the role of TLR4 in diabetic glomerulopathy or hyperlipidaemia-induced kidney damage remains to be elucidated [8–13]. Recently, Burkhardt et al and Bouma et al reported that serum S100A8/A9 complex concentrations were elevated in patients with diabetes [33, 34]. In our study, S100A8 protein was abundant in the glomeruli of mice given STZ and HFD and also in glomeruli of patients with diabetic nephropathy, and was mainly produced by macrophages. Furthermore, we found that high glucose and NEFA treatments, when combined, markedly upregulated *S100a8* expression in WT macrophages, but not in *Tlr4* KO macrophages. These findings suggest that production of S100A8 is not just an indicator of systemic inflammation but may play a pathogenic role in the deterioration of diabetic nephropathy. Functional analysis of S100A8 protein production in diabetic mice is currently under way in our laboratory. Candidate *Tlr4*-expressing cells in the diabetic kidney include macrophages, podocytes and mesangial and tubular epithelial cells [8, 9]. So far, we have been unable to obtain reliable findings by immunohistochemistry using commercially available antibodies for TLR4, and we are now trying other methods. Of note, upregulation of *S100a8* gene expression by HFD in STZ mice was also observed in the liver and aorta, suggesting that the effects of these treatments are not specifically targeted to the kidney but are systemic (ESM Fig. 6). HMGB1 is one of endogenous ligands of TLR4 [9], and AGE-specific receptor (AGER or RAGE) is one of the S100A8 receptors so far identified [35]. Although mRNA expression of these molecules in glomeruli was not upregulated in diabetic mice in this study (ESM Fig. 3, ESM Table 4), we cannot exclude the possibility that they are involved in hyperlipidaemia-induced renal injury.

The macrophage has been presumed to be a critical mediator of diabetic nephropathy [36–38], and blockade of the MCP-1/CC chemokine receptor 2 system in diabetic mice leads to reduced albuminuria, mesangial expansion and macrophage infiltration [39–42]. Secretory factors from macrophages may cause histological and functional changes in glomeruli. For example, TGF β1 (TGFB1) and MCP1, induced in surrounding cells by or secreted directly from activated macrophages, have been shown to upregulate CTGF production [43] and increase albumin permeability in cultured podocytes [44–46]; we have recently reported that overproduction of CTGF specifically in podocytes is sufficient to worsen diabetic nephropathy [19].

Downstream signalling of TLR4 has been divided into MYD88-dependent and TRIF-dependent pathways, leading to early- and late-phase nuclear factor of κ light polypeptide gene enhancer in B cells 1 (NFκB) activation, respectively [7]. In addition, endocytosed TLR4 activates the TRIF-dependent pathway [47]. It is interesting to determine whether pathologically accumulated lipids in endosomes of macrophages can cause chronic inflammation via the TRIF-dependent pathway in the kidneys of STZ-HFD mice. Here, in STZ-HFD kidneys, we observed an increase in IRF3 protein phosphorylation and *Cxcl10*, *Ifnb1* and *Cd80* mRNA expression, reported to be in the TRIF-dependent pathway, but experiments blocking TRIF activity are required to demonstrate the TRIF dependency of the process.

In conclusion, we have elucidated a novel mechanism of hyperlipidaemia-induced renal damage in diabetic conditions in a TLR4-dependent manner that appears to involve the activation of a S100A8/TLR4 signalling pathway in glomeruli. Further investigation is required to see whether this signalling cascade is relevant in the progression of nephropathy in diabetic patients.

Acknowledgements We acknowledge S. Akira (WPI Immunology Frontier Research Center, Osaka University, Suita, Japan) for kindly providing us with *Tlr4* KO mice. We gratefully acknowledge Y. Ogawa and A. Yamamoto and other laboratory members for their assistance.

Funding This work was supported in part by Grant-in-Aid for Diabetic Nephropathy Research (K. Mori), research grants from the Japanese Ministry of Education, Culture, Sports, Science and Technology (T. Kuwabara, K. Mori and M. Mukoyama) and from the Smoking Research Foundation (M. Mukoyama).

Duality of interest The authors declare that there is no duality of interest associated with this manuscript.

Contribution statement All authors contributed to the conception and design, or analysis and interpretation of data, and drafting the article or revising it critically for important intellectual content, and have given final approval of the version to be published.

References

1. Maisonneuve P, Agodoa L, Gellert R et al (2000) Distribution of primary renal diseases leading to end-stage renal failure in the United States, Europe, and Australia/New Zealand: results from an international comparative study. Am J Kidney Dis 35:157–165
2. Decleves AE, Sharma K (2010) New pharmacological treatments for improving renal outcomes in diabetes. Nat Rev Nephrol 6:371–380
3. El-Atat FA, Stas SN, McFarlane SI, Sowers JR (2004) The relationship between hyperinsulinemia, hypertension and progressive renal disease. J Am Soc Nephrol 15:2816–2827
4. Perkins BA, Ficociello LH, Silva KH, Finkelstein DM, Warram JH, Krolewski AS (2003) Regression of microalbuminuria in type 1 diabetes. N Engl J Med 348:2285–2293
5. Ravid M, Brosh D, Ravid-Safran D, Levy Z, Rachmani R (1998) Main risk factors for nephropathy in type 2 diabetes mellitus are plasma cholesterol levels, mean blood pressure, and hyperglycemia. Arch Intern Med 158:998–1004
6. Rutledge JC, Ng KF, Aung HH, Wilson DW (2010) Role of triglyceride-rich lipoproteins in diabetic nephropathy. Nat Rev Nephrol 6:361–370

7. Akira S, Takeda K (2004) Toll-like receptor signalling. Nat Rev Immunol 4:499–511
8. Brown HJ, Lock HR, Wolfs TG, Buurman WA, Sacks SH, Robson MG (2007) Toll-like receptor 4 ligation on intrinsic renal cells contributes to the induction of antibody-mediated glomerulonephritis via CXCL1 and CXCL2. J Am Soc Nephrol 18:1732–1739
9. Wu H, Chen G, Wyburn KR et al (2007) TLR4 activation mediates kidney ischemia/reperfusion injury. J Clin Invest 117:2847–2859
10. Zhang B, Ramesh G, Uematsu S, Akira S, Reeves WB (2008) TLR4 signaling mediates inflammation and tissue injury in nephrotoxicity. J Am Soc Nephrol 19:923–932
11. Liu B, Yang Y, Dai J et al (2006) TLR4 up-regulation at protein or gene level is pathogenic for lupus-like autoimmune disease. J Immunol 177:6880–6888
12. Kruger B, Krick S, Dhillon N et al (2009) Donor Toll-like receptor 4 contributes to ischemia and reperfusion injury following human kidney transplantation. Proc Natl Acad Sci USA 106:3390–3395
13. Lin M, Yiu WH, Wu HJ et al (2012) Toll-like receptor 4 promotes tubular inflammation in diabetic nephropathy. J Am Soc Nephrol 23:86–102
14. Hoshino K, Takeuchi O, Kawai T et al (1999) Cutting edge: Toll-like receptor 4 (TLR4)-deficient mice are hyporesponsive to lipopolysaccharide: evidence for TLR4 as the Lps gene product. J Immunol 162:3749–3752
15. Kuwabara T, Mori K, Mukoyama M et al (2009) Urinary neutrophil gelatinase-associated lipocalin levels reflect damage to glomeruli, proximal tubules, and distal nephrons. Kidney Int 75:285–294
16. Kusakabe T, Tanioka H, Ebihara K et al (2009) Beneficial effects of leptin on glycaemic and lipid control in a mouse model of type 2 diabetes with increased adiposity induced by streptozotocin and a high-fat diet. Diabetologia 52:675–683
17. Jung K, Wesslau C, Priem F, Schreiber G, Zubek A (1987) Specific creatinine determination in laboratory animals using the new enzymatic test kit "Creatinine-PAP". J Clin Chem Clin Biochem 25:357–361
18. Suganami T, Mukoyama M, Sugawara A et al (2001) Overexpression of brain natriuretic peptide in mice ameliorates immune-mediated renal injury. J Am Soc Nephrol 12:2652–2663
19. Yokoi H, Mukoyama M, Mori K et al (2008) Overexpression of connective tissue growth factor in podocytes worsens diabetic nephropathy in mice. Kidney Int 73:446–455
20. Suganami T, Mukoyama M, Mori K (2005) Prevention and reversal of renal injury by leptin in a new mouse model of diabetic nephropathy. FASEB J 19:127–129
21. Suganami T, Yuan X, Shimoda Y et al (2009) Activating transcription factor 3 constitutes a negative feedback mechanism that attenuates saturated Fatty acid/toll-like receptor 4 signaling and macrophage activation in obese adipose tissue. Circ Res 105:25–32
22. Qi Z, Fujita H, Jin J et al (2005) Characterization of susceptibility of inbred mouse strains to diabetic nephropathy. Diabetes 54:2628–2637
23. Vaisse C, Halaas JL, Horvath CM, Darnell JE Jr, Stoffel M, Friedman JM (1996) Leptin activation of Stat3 in the hypothalamus of wild-type and ob/ob mice but not db/db mice. Nat Genet 14:95–97
24. Vogl T, Tenbrock K, Ludwig S et al (2007) Mrp8 and Mrp14 are endogenous activators of Toll-like receptor 4, promoting lethal, endotoxin-induced shock. Nat Med 13:1042–1049
25. Suganami T, Mieda T, Itoh M, Shimoda Y, Kamei Y, Ogawa Y (2007) Attenuation of obesity-induced adipose tissue inflammation in C3H/HeJ mice carrying a Toll-like receptor 4 mutation. Biochem Biophys Res Commun 354:45–49
26. Shi H, Kokoeva MV, Inouye K, Tzameli I, Yin H, Flier JS (2006) TLR4 links innate immunity and fatty acid-induced insulin resistance. J Clin Invest 116:3015–3025
27. Xu XH, Shah PK, Faure E et al (2001) Toll-like receptor-4 is expressed by macrophages in murine and human lipid-rich atherosclerotic plaques and upregulated by oxidized LDL. Circulation 104:3103–3108
28. Kume S, Uzu T, Araki S et al (2007) Role of altered renal lipid metabolism in the development of renal injury induced by a high-fat diet. J Am Soc Nephrol 18:2715–2723
29. Okamura DM, Pennathur S, Pasichnyk K et al (2009) CD36 regulates oxidative stress and inflammation in hypercholesterolemic CKD. J Am Soc Nephrol 20:495–505
30. Jiang T, Wang Z, Proctor G et al (2005) Diet-induced obesity in C57BL/6J mice causes increased renal lipid accumulation and glomerulosclerosis via a sterol regulatory element-binding protein-1c-dependent pathway. J Biol Chem 280:32317–32325
31. Croce K, Gao H, Wang Y et al (2009) Myeloid-related protein-8/14 is critical for the biological response to vascular injury. Circulation 120:427–436
32. Loser K, Vogl T, Voskort M et al (2010) The Toll-like receptor 4 ligands Mrp8 and Mrp14 are crucial in the development of autoreactive CD8+ T cells. Nat Med 16:713–717
33. Burkhardt K, Schwarz S, Pan C et al (2009) Myeloid-related protein 8/14 complex describes microcirculatory alterations in patients with type 2 diabetes and nephropathy. Cardiovasc Diabetol 8:10
34. Bouma G, Lam-Tse WK, Wierenga-Wolf AF, Drexhage HA, Versnel MA (2004) Increased serum levels of MRP-8/14 in type 1 diabetes induce an increased expression of CD11b and an enhanced adhesion of circulating monocytes to fibronectin. Diabetes 53:1979–1986
35. Yamamoto Y, Kato I, Doi T et al (2001) Development and prevention of advanced diabetic nephropathy in RAGE-overexpressing mice. J Clin Invest 108:261–268
36. Furuta T, Saito T, Ootaka T et al (1993) The role of macrophages in diabetic glomerulosclerosis. Am J Kidney Dis 21:480–485
37. Sassy-Prigent C, Heudes D, Mandet C et al (2000) Early glomerular macrophage recruitment in streptozotocin-induced diabetic rats. Diabetes 49:466–475
38. Usui HK, Shikata K, Sasaki M et al (2007) Macrophage scavenger receptor-a-deficient mice are resistant against diabetic nephropathy through amelioration of microinflammation. Diabetes 56:363–372
39. Chow FY, Nikolic-Paterson DJ, Ozols E, Atkins RC, Rollin BJ, Tesch GH (2006) Monocyte chemoattractant protein-1 promotes the development of diabetic renal injury in streptozotocin-treated mice. Kidney Int 69:73–80
40. Chow FY, Nikolic-Paterson DJ, Ma FY, Ozols E, Rollins BJ, Tesch GH (2007) Monocyte chemoattractant protein-1-induced tissue inflammation is critical for the development of renal injury but not type 2 diabetes in obese db/db mice. Diabetologia 50:471–480
41. Kanamori H, Matsubara T, Mima A et al (2007) Inhibition of MCP-1/CCR2 pathway ameliorates the development of diabetic nephropathy. Biochem Biophys Res Commun 360:772–777
42. Sayyed SG, Ryu M, Kulkarni OP et al (2011) An orally active chemokine receptor CCR2 antagonist prevents glomerulosclerosis and renal failure in type 2 diabetes. Kidney Int 80:68–78
43. Yokoi H, Mukoyama M, Sugawara A et al (2002) Role of connective tissue growth factor in fibronectin expression and tubulointerstitial fibrosis. Am J Physiol Renal Physiol 282:F933–942
44. Takano Y, Yamauchi K, Hayakawa K et al (2007) Transcriptional suppression of nephrin in podocytes by macrophages: roles of inflammatory cytokines and involvement of the PI3K/Akt pathway. FEBS Lett 581:421–426
45. Lee EY, Chung CH, Khoury CC et al (2009) The monocyte chemoattractant protein-1/CCR2 loop, inducible by TGF-beta, increases podocyte motility and albumin permeability. Am J Physiol Renal Physiol 297:F85–94
46. Kwoh C, Shannon MB, Miner JH, Shaw A (2006) Pathogenesis of nonimmune glomerulopathies. Annu Rev Pathol 1:349–374
47. Kagan JC, Su T, Horng T, Chow A, Akira S, Medzhitov R (2008) TRAM couples endocytosis of Toll-like receptor 4 to the induction of interferon-beta. Nat Immunol 9:361–368